

FLAT SLAB PUNCHING BEHAVIOUR UNDER CYCLIC HORIZONTAL LOADING

André Almeida, Micael Inácio, Válder Lúcio, António Pinho Ramos

Department of Civil Engineering, Faculdade de Ciências e Tecnologia, Universidade NOVA de Lisboa, 2829-516 Caparica, Portugal

Abstract

This experimental work aims to study the behaviour of reinforced concrete flat slabs, without shear reinforcement, under gravity and horizontal loading. The effect of gravity load ratio, drift amplitude and horizontal loading nature (cyclic or monotonic) were the studied variables, to ascertain its influence in load and drift capacity, as well the slab-column connection degradation. To accomplish this, four similar flat slab specimens, measuring $4.15 \times 1.85 \times 0.15 \text{m}^3$, were tested under different test protocols, using an innovative test setup whose boundary conditions better approximate laboratory specimens to reality. The obtained results show that cyclic horizontal loads are extremely detrimental to the slab-column connection. The observed drift capacity is not satisfactory, even under low gravity loads.

Keywords: Cyclic Load, Experimental Work, Flat Slab, Punching, Reinforced Concrete

1 Introduction

For the last decades, the architectural and economic advantages of flat slab buildings make them the primary choice for both habitation and office buildings. Its main benefit, the absence of beams leads to its main weakness, the possible occurrence of a punching failure. Although this is a widely studied phenomenon, punching under cyclic horizontal loading still is a not well known subject by the scientific community. Because of its complexity, a huge amount of experimental tests are needed to assort the influence of each one of the phenomenon's many variables in the slab's behaviour.

The majority of the experimental tests performed to study this subject are simplified representations of slab-column connections. Although, very practical and laboratory friendly because their simplified boundary conditions, those tests do not represent well the real phenomenon. In this experimental work, more realistic boundary conditions were used to ensure a non-zero bending moment at mid-span and consequently a non-fixed null bending moment line.

2 Experimental campaign

2.1 Specimens' description

The specimens were designed in order to represent a slab-column connection of an ordinary office building. Their measurements are 4.15m in the longitudinal direction (N-S), 1.85m in the transversal direction (E-W) and 0.15m thick. The average reinforcement ratio at the column was around 1.0% and its design schematics are shown in Figure 1. To ease the specimens' production, transportation and handling, a steel column was used. The linear elastic properties of the column also simplify the results analysis.

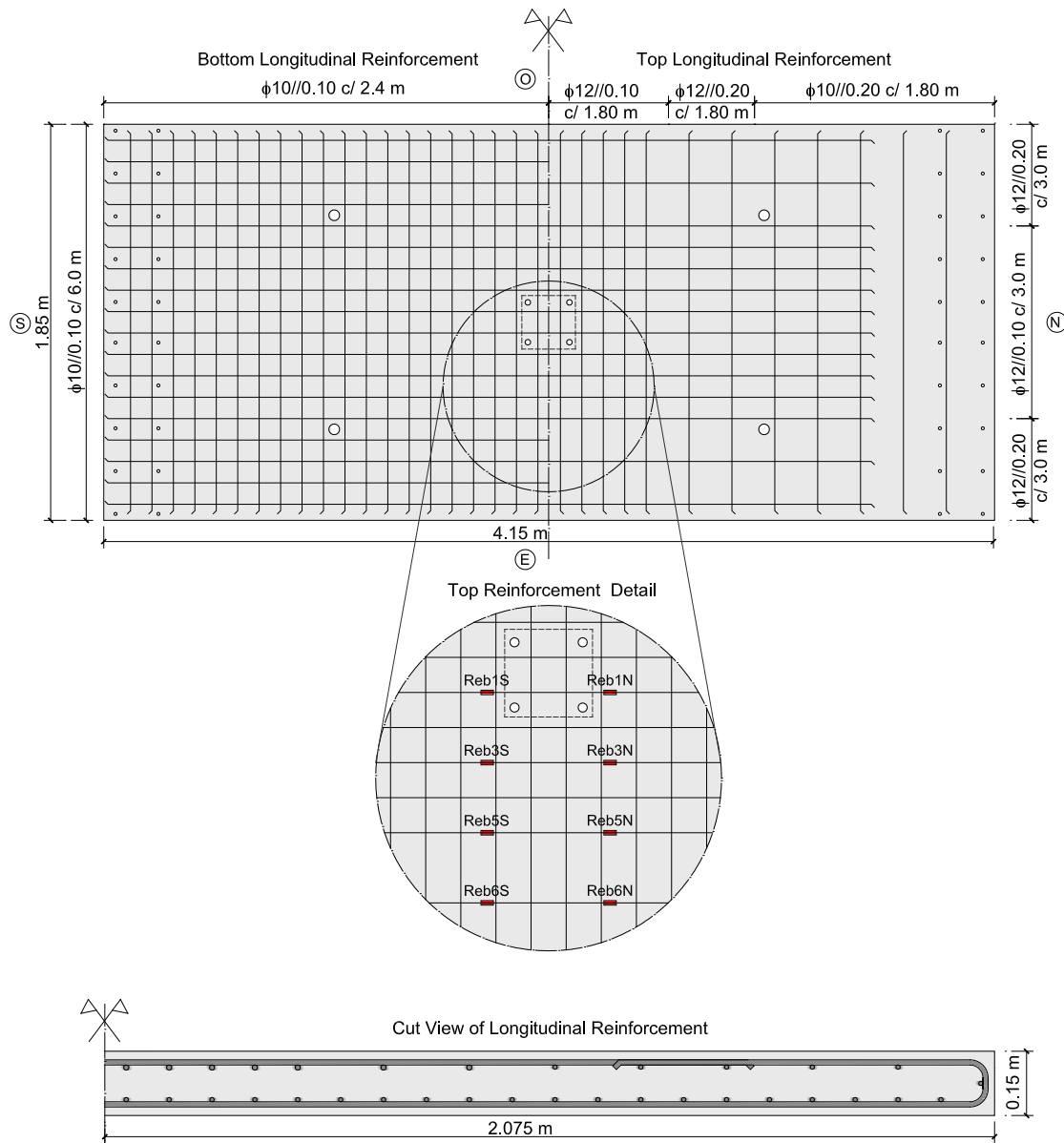


Figure 1 – Detail of the reinforcement and strain gauges position

2.2 Test setup and instrumentation

The cyclic nature of the action makes it difficult to faithfully replicate in laboratory conditions. The commonly used test setups [3-5, 7-14] fails to ensure two relevant boundary conditions: the zero bending moment line mobility and equal shear force at the N-S border, due to the cyclic horizontal action.

Trying to approximate the laboratory conditions to reality, a new test setup was developed, with the following conditions in mind: for gravity load only, shear forces and rotations at the N-S borders are null and the vertical displacements as well as bending moments are equal, as should be at the slab's mid-span; when cyclic horizontal loads take place, rotations, vertical displacements and shear forces at the N-S borders should be equal in magnitude.

To do so, a combination of two passive systems was used. Two double pinned struts connecting the two borders granted the bending moment and rotation to be similar, while four seesaw like elements took care of the vertical displacements and shear forces equality. All the elements from those systems were designed to be rigid so they do not interfere with the test results.

The gravity load was applied by four hydraulic jacks, connected to a load maintainer machine, allowing high gravity loads to be kept constant throughout the test. The applied gravity load reacted with the bottom steel column instead of the laboratory's strong floor to allow the specimen's horizontal movements. Figure 2 shows the test setup.



Figure 2 – Test setup

Eighteen displacement transducers were used, fourteen along the N-S direction and four across the E-W direction, to measure vertical displacement relatively to the top column's base. The horizontal displacement at the column's top was measured by a long range LVDT. Eight pairs of strain gauges, placed as shown in Figure 1 (detail), were used to monitor the top longitudinal reinforcement's strains during the test. Each hydraulic jack used to apply the gravity load had its own load cell, to both quantify the applied load and assure it was evenly distributed. The mechanical actuator responsible for the horizontal displacement had a dedicated load cell. The top and bottom steel columns' bases are solid steel plates with 250x250x50mm³, pre-stressed against the slab by four M24 bolts.

2.3 Materials

All specimens were cast at a precast facility. From each specimen, 150mm side cubes and 300mm long cylinders with 150mm diameter were also cast. The mean compressive strength in cubes ($f_{cm,cube}$) was obtained by testing six cubes for every specimen. This value was then used to calculate the mean compressive strength (f_{cm}) by multiplying $f_{cm,cube}$ by 0.8. The mean splitting tensile strength ($f_{ct,sp}$) was obtained by testing three cylinders to Splitting Test. Tensile tests were also performed on steel coupons from the same batch as the ones used in the slabs. Table 1 summarizes the concrete characteristics, along with the yield strength of the reinforcement (f_y).

Table 1 – Concrete and steel characteristics

Specimen	$f_{cm,cube}$ [MPa]	f_{cm} [MPa]	$f_{ct,sp}$ [MPa]	f_y [MPa]		ϵ_y [%]
				$\phi 10$	$\phi 12$	
E-50	56.7	45.3	-			
C-50	50.3	38.9	2.9	532.9	534.6	0.26
C-40	52.7	42.2	4.2			
C-30	61.2	49.0	4.3			

2.4 Test protocol

Two different test protocols were used, according to the horizontal loading nature. For the monotonic eccentricity test, a gravity load was applied at a rate of 15kN/min until the target load was achieved and then kept constant, and afterwards an increasing horizontal displacement was imposed at the top of the column at a 1.25mm/min speed. The cyclic eccentricity tests consisted in gravity loading the specimen at a rate of 30kN/min, until a target load was reached. Then, starting in the N-S direction, a cyclic horizontal displacement of 9.2mm/min was induced at the column top, according to the protocol shown in Figure 3.

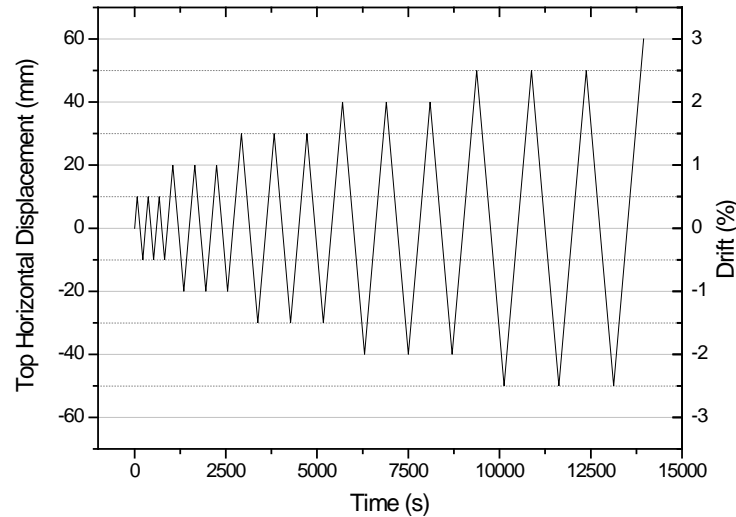


Figure 3 – Cyclic tests' horizontal displacement protocol

The target gravity load applied by the hydraulic jacks for each specimen was a percentage of the EC2 [15] provision, as shown in Table 2, from which 39.4kN was subtracted corresponding to specimens and test setup self-weight. Table 2 shows each test's main characteristics.

Table 2 – Test characteristics

Specimen	d [mm]	ρ [%]	V_{Rc} (EC2) [kN]	Eccentricity	Gravity Load
E-50	117.6	0.96	425.3	Monotonic	$0.5 V_{Rc}$
C-50	118.4	0.96	406.9	Cyclic	$0.5 V_{Rc}$
C-40	118.3	0.96	418.4	Cyclic	$0.4 V_{Rc}$
C-30	117.9	0.96	437.7	Cyclic	$0.3 V_{Rc}$

3 Test results

The test setup worked as expected. Vertical displacements and shear forces were well matched both for gravity and horizontal loading test phases. The rotation and bending moment imposition mechanism worked as well. Vertical displacement increased for cycles under the same drift step and bending cracks appeared at slabs' soffit, at mid-span, showing the presence of positive bending moments in that region. Inflection points were also visible in the slab's deformed shape. Regarding the steel column behaviour, no issues were observed such as column decompression, sliding or concrete crushing underneath.

The specimen subjected to monotonic eccentricity, E-50, presented negative bending moment cracking along the E-W for the target gravity load (212.7kN), although, strain gauges at the top reinforcement rebars show no yielding at that load stage..

After gravity load was applied, an increasing monotonic horizontal displacement was imposed in the N-S direction. The presence of unbalanced bending moment was observed through the strain gauges' data. A strain increase at the North side was observed, opposed to a strain decrease at the South side resulting in a more prominent cracking at the North side and crack closing at the South side of the slab. When a drift of about 1.0% was reached, top longitudinal reinforcement under the column experienced a stress signal inversion, going into a compression state. This phenomenon was not observed for rebars farther from the column, which indicates that unbalanced moment is absorbed in the column's vicinity. For higher eccentricities, several top longitudinal rebars yielded at the North side of the column. The Horizontal Load-Top Horizontal Displacement chart depicted in Figure 4 shows stiffness loss until a brittle punching failure was reached for about 1.8% drift.

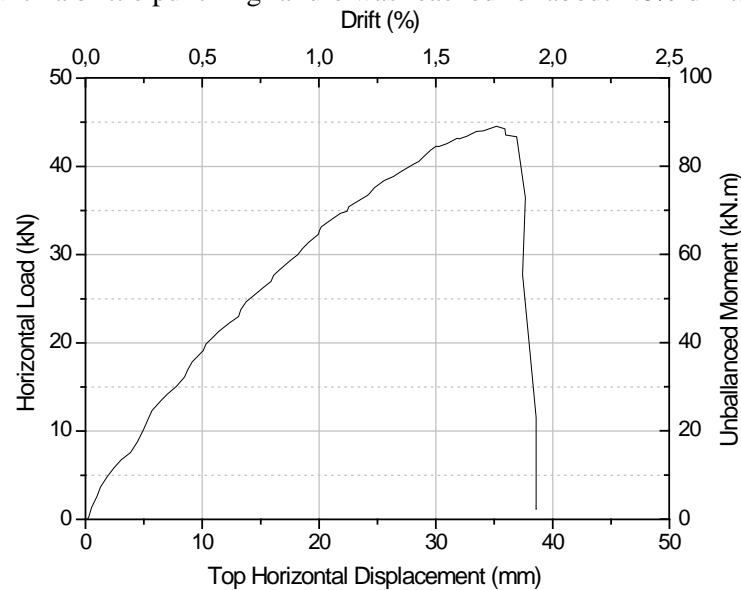


Figure 4 – E-50. Horizontal load Vs horizontal displacement

The remaining slabs were tested using the cyclic eccentricity test protocol. Specimens C-50, C-40 and C-30 were gravity loaded until 203.4kN, 167.4kN and 131.3kN respectively, according to the stipulated shear ratio (Table 2). All specimens presented visible cracking due to negative bending moment at the column for the target load but none of their reinforcement show signs of yielding at that stage.

Following the protocol, the cycles began in the N-S direction. Both C-50 and C-40 specimens presented yielding at the top rebars under the column for the first complete cycles for both North and the South sides, while C-30 specimen showed rebar yielding starting for the 1.0% cycles only. The lower the shear ratio, the higher the cycle step for which yielding occurred. Lower shear ratios also increased the capacity to spread the unbalanced moment along a wider area around the column. The C-30 specimen presented an almost even stress distribution for all longitudinal rebars, except for the ones under the column. The cyclic nature of the horizontal load was visible in the strain gauges that show that the stresses at rebars experience cyclic behaviour. The peak stress at rebars gradually increased throughout the test due to the increasing slabs' deformation due to combined action of gravity and cyclic horizontal loads.

Slabs' stiffness degradation was noticeable at each drift step but also between different cycles under the same step, although, less pronounced. The lower the shear ratio, the more drift the specimen could withstand until punching failure occurred.

Hysteretic diagrams depicted in Figures 5 to 7 show that all C-50, C-40 and C-30 specimens had a low energy dissipation capacity. Stiffness loss is negligible for cycles up to 1.0% drift. Viscous damping coefficients for each model were calculated as suggested by Seible [16]. All specimens presented a viscous damping coefficient under 10% which according to the author [16], means almost elastic behaviour and, therefore, low energy dissipation capacity.

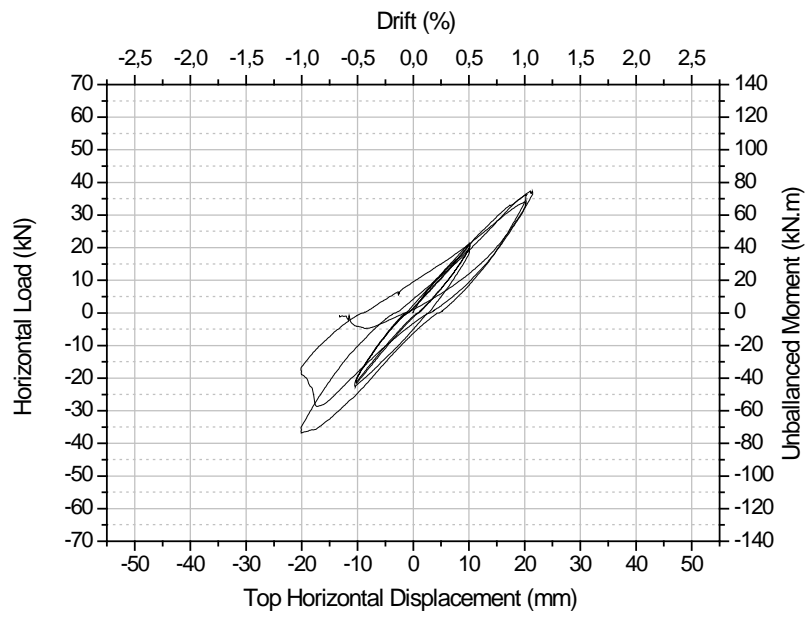


Figure 5 – C-50. Hysteretic diagram

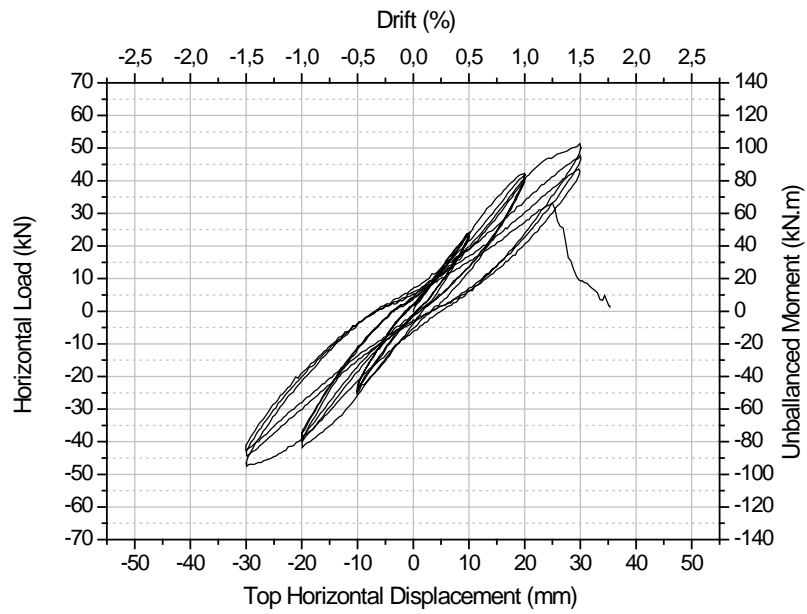


Figure 6 - C-40. Hysteretic diagram

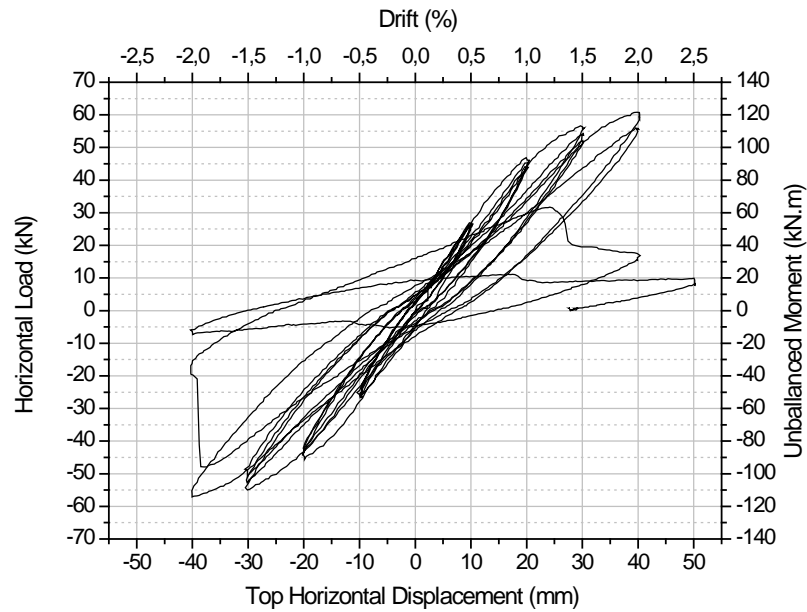


Figure 7 - C-30. Hysteretic diagram

EC2's formulation for eccentric punching was applied for all specimens. Results presented in Table 3 show that the EC2 provisions are fairly accurate, although, non-conservative for the C-50 specimen.

Table 3 – EC2's eccentric punching formulation

Specimen	M_{exp} [kN.m]	β	V_{rc} [kN]	βV_{exp} [kN]	$\beta V_{exp} / V_{rc}$
E-50	90.6	2.06	425.3	439.2	1.03
C-50	74.7	1.91	406.9	389.3	0.96
C-40	109.3	2.62	418.4	439.3	1.05
C-30	122.6	3.33	437.7	437.2	1.00

This formulation, however, when used with elastic moments, is very conservative, which is not applicable for design purposes. The real unbalanced bending moment calculation is a non-linear complex process and for this reason, it is also difficult to predict the slab's drift capacity. It is important to ensure drift capacity taking advantage of the slab's stiffness loss.

4 Conclusions

This paper describes the experimental work developed at FCT/UNL to study the behaviour of flat slab under gravity and horizontal cyclic loads. The main conclusions are:

1. The test setup accomplished its goals. The vertical displacements were matched and shear forces at the border were symmetrical as intended. The moment and rotation compatibilization system presented good results. Positive bending moment cracks at the north and south border also proved the system's effectiveness.
2. The gravity load system was proven effective in both maintaining the load constant throughout the test and spread the load evenly at the slab's surface.
3. The achieved drift capacity grows in inverse proportion to the gravity load ratio.
4. Cyclic action induces severe damage to the slab-column connection. It was observed that vertical displacement at the slab's border for the third 0.5% drift cycle of the C-50 specimen was of the same magnitude of the pre-failure vertical displacement of the E-50 specimen (1.8% drift).
5. No rebars yielded for gravity load only.
6. When horizontal action takes place, rebars under the column are the most stressed, yielding in the first cycles when pulled. For higher drift steps (1.0%) those rebars experienced a stress signal

inversion when compressed.

7. Strain gauges show that the unbalanced moment is absorbed in the column's vicinity. Lower shear ratios also increased the capacity to spread the unbalanced moment along a wider area around the column.
8. EC2's formulation for eccentric punching predicts satisfactorily the supported unbalanced moment, however, using it to predicting drift capacity is a very complex task.

Acknowledgements

The author wishes to acknowledge the support of Fundação para a Ciência e a Tecnologia – Ministério da Educação e Ciência, through Project EXPL/ECM – EST/1371/2013

References

- [1] Robertson, I. *et al* (1990), Seismic Response Of Connections in Indeterminate Flat-Slab Subassemblies, PhD Thesis, William Mash Rice University
- [2] Diaz, A. J.(1991), Seismic Resistance of Fiber-Reinforced Slab-Column Connections, William Mash Rice University
- [3] Soares, J. (1993), Punçoamento Excêntrico em Lajes Fungiformes de Betão Armado, MSc Thesis, Universidade Técnica de Lisboa
- [4] Tegos, J. and Tsonos, A. (1996), Punching Strength Decay of Slab-Column Connections Under Seismic Loading, Elsevier Science Ltd. Paper No. 654. Eleventh World Conference on Earthquake Engineering
- [5] Stark, A. *et al* (2004), Seismic Upgrade of Slab-Column Connection Using Carbon Fiber Reinforcement, Paper No. 102, 13 WCEE Vancouver, B.C., Canada, August 1-6, 2004
- [6] Coelho, E. *et al* (1994), Assessment of the Seismic Behaviour of RC Flat Slab Building Structures, Paper No. 2630, 13th World Conference on Earthquake Engineering, Vancouver, B.C., Canada
- [7] Tandian, C.H. and Warnitchai, P. (2008), Seismic performance enhancement of post-tensioned flat plate systems with drop panel, Asian Institute of Technology, Thailand
- [8] Anggadajaja, E., Teng S., Edge-column slab connections under gravity and lateral loading, ACI Structural Journal, V. 105, N° 5, USA, 2008, pp. 541-551.
- [9] Cheng e Parra-Montesinos (2010), Evaluation of Steel Fiber Reinforcement for Punching Shear Resistance in Slab-Column Connections, ACI Structural Journal, V. 107, N° 2, USA, 2010, pp. 110-118
- [10] Widianto (2010), Seismic Rehabilitation of Slab-Column Connections, ACI Structural Journal, V. 107, N° 2, USA, 2010, pp. 237-247
- [11] Vollum, A. (2011), Performance of Ductile RC Flat Slab to Steel Column Connections Under Cyclic Loading, Engineering Structures 36 (2012) 239–257
- [12] Bu, W. (2008), Punching Shear Retrofit Method Using Shear Bolt For Reinforced Concrete Slabs Under Seismic Loading, PhD Thesis, University of Waterloo

- [13] Robertson, I. *et al* (2002), Cyclic Testing of Slab-Column Connections With Shear Reinforcement, ACI Structural Journal, V. 99, N° 5, USA, 2002, pp. 605-613
- [14] Kang, T., Wallace, J., Seismic performance of reinforced concrete slab-column connections with plate stirrups, ACI Structural Journal, V. 105, N° 5, USA, 2008, pp. 617-625.
- [15] European Committee for Standardization, EN 1992-1-1 Eurocode 2: design of concrete structures – Part 1-1: general rules and rules for buildings, 2004.
- [16] Hose, Y. D. and Seible, F. (1999). Performance evaluation database for concrete bridge components and systems under simulated seismic loads. Technical Report PEER 1999/11, Pacific Earthquake Engineering Research Center.
- [17] Marreiros, R. (2014) Precast Concrete Wall-Foundation Connection - Development of a seismic dissipative connection, PhD Thesis, FCT/Universidade Nova de Lisboa.